APPROXIMATE ANALYSIS OF SURFACE WAVE-STRUCTURE INTERACTION

Nihal Ege, Bariş Erbaş, Julius Kaplunov and Peter Wootton

msp

APPROXIMATE ANALYSIS OF SURFACE WAVE-STRUCTURE INTERACTION

Nihal Ege, Barış Erbaş, Julius Kaplunov and Peter Wootton

Surface wave-structure interaction is studied starting from a specialised approximate formulation involving a hyperbolic equation for the Rayleigh wave along with pseudostatic elliptic equations over the interior of an elastic half-space. The validity of the proposed approach for modelling a point contact is analysed. Explicit dispersion relations are derived for smooth contact stresses arising from averaging the effect of a regular array of spring-mass oscillators and also of elastic rods attached to the surface. Comparison with the exact solution of the associated plane time-harmonic problem in elasticity for the array of rods demonstrates a high efficiency of the developed methodology.

1. Introduction

Dynamic soil-structure interaction was investigated in great detail in numerous publications (for examples, see the widely cited book [Wolf 1985] and general reference work [Luco 1982]) with the emphasis usually placed on the effect of bulk waves, in particular in the insightful papers by Boutin and Roussillon [2004; 2006]. Seemingly surface wave-structure interaction has not been studied until very recently when it has been motivated by seismic metasurfaces design, see [Colombi et al. 2016; Colquitt et al. 2017], in which an array of rods attached to the surface of an elastic half-space is analysed starting from full dynamic equations in linear elasticity.

In this paper, a specialized surface wave model, e.g., see [Kaplunov and Prikazchikov 2013; 2017], is adapted for a broad range of soil-structure interaction problems. The mathematical formulation consists of an explicit wave equation on the surface along with pseudostatic elliptic equations governing the decay over the interior. Although the model has been previously implemented to a variety of dynamic scenarios, including 3D moving load problems [Kaplunov et al. 2013; Erbaş et al. 2017], its validity for studying soil-structure interaction is not immediately obvious. The point is that the asymptotic theory exposed in [Kaplunov and Prikazchikov 2013; 2017] is oriented to near-resonance excitation in the form of a prescribed wave disturbance with the phase speed close to the Rayleigh wave one. Thus, for soil-structure interaction problems involving unknown contact stresses, the assumption of near-resonance behaviour always has to be verified *a posteriori*.

The paper is organized as follows: 3D equations governing transient surface wave-structure interaction are presented in Section 2. For the sake of simplicity, structure dynamics is modelled by a scalar partial differential equation in vertical displacement, which is specified in what follows. In Section 3, a plane

point time-harmonic contact is considered. It is demonstrated that the approximate surface wave model is not applicable due to presence of a spurious localized component. At the same time, the sought after Rayleigh wave contribution predicted by this model is identical to that within the exact solution of the plane time-harmonic problem given in the Appendix.

The effect of smooth contact surface stresses coming from homogenizing regular arrays of resonators attached to the surface of a half-space is studied in Sections 4 and 5. The simplest spring-mass resonators are considered in Section 4, while the next section deals with an array of elastic rods. Explicit dispersion relations are readily derived in both cases. Comparison of the approximate solution in Section 5 with the exact solution presented in [Colquitt et al. 2017] shows a remarkable similarity.

2. Statement of the problem

Let us study dynamic interaction of an elastic structure and a homogeneous isotropic half-space, see Figure 1, starting from the earlier proposed asymptotic model for surface wave fields, e.g., see [Kaplunov and Prikazchikov 2017]. According to this model, we have for the longitudinal wave potential φ the hyperbolic equation

$$\Delta_2 \varphi - \frac{1}{c_R^2} \varphi_{tt} = \frac{(1+k_2^2)}{2\mu B} P \tag{2-1}$$

at the contact surface $x_3 = 0$ along with the elliptic equation

$$\frac{\partial^2 \varphi}{\partial x_3^2} + k_1^2 \Delta_2 \varphi = 0 \tag{2-2}$$

over the interior $(-\infty < x_1, \ x_2 < \infty, \ 0 < x_3 < \infty)$, where

$$k_i^2 = 1 - \frac{c_R^2}{c_i^2}, \quad i = 1, 2,$$

and

$$B = \frac{k_1}{k_2}(1 - k_2^2) + \frac{k_2}{k_1}(1 - k_1^2) - (1 - k_2^4).$$

In the formulae above, t is time, c_1, c_2, and c_R are the longitudinal, shear, and Rayleigh wave speeds, respectively, μ is the Lamé constant, $P = P(x_1, x_2, t)$ is the unknown normal contact stress, $\Delta_2 = \partial^2/\partial x_1^2 + \partial^2/\partial x_2^2$. The displacement vector is expressed through the longitudinal and shear potentials φ
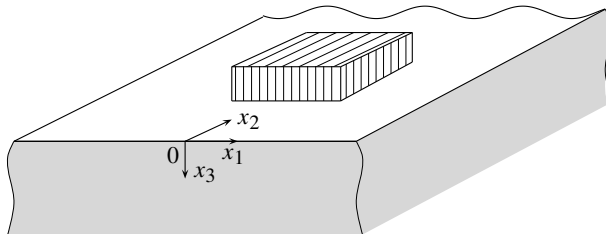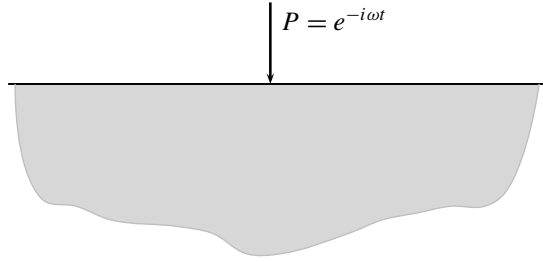

Figure 1. Elastic solid-structure interaction.

Figure 2. Point time-harmonic force.

and $\boldsymbol{\psi}$ as

$$\boldsymbol{u} = (u_1, u_2, u_3) = \operatorname{grad} \varphi + \operatorname{curl} \boldsymbol{\psi}, \tag{2-3}$$

where

$$\boldsymbol{\psi} = (-\psi_2, \psi_1, 0),$$

with its components satisfying the equations

$$\frac{\partial^2 \psi_i}{\partial x_3^2} + k_2^2 \Delta_2 \psi_i = 0, \quad i = 1, 2, \tag{2-4}$$

over the surface $x_3 > 0$ and the conditions

$$\frac{\partial \psi_i}{\partial x_3} = \frac{1 + k_2^2}{2} \frac{\partial \varphi}{\partial x_i} \tag{2-5}$$

at the interface $x_3 = 0$.

For the sake of simplicity, we model the dynamic behaviour of an elastic structure, see Figure 1, by the following scalar equation:

$$Lv = mv_{tt} \tag{2-6}$$

over the region $-\infty < x_1, x_2 < \infty$, $-\infty < x_3 < 0$, where $v(x_k, t)$, $k = 1, 2, 3$ is the vertical displacement, m is the mass, and L is a symbolic notation for a differential operator in the variables x_k. The contact conditions at $x_3 = 0$ are taken in the form

$$P = lv \quad \text{and} \quad v = u_3, \tag{2-7}$$

where l also denotes a differential operator in x_k. The presented formulation is oriented to the scenario with a dominant contribution of surface waves to the overall dynamic response. In this case, the effect of bulk waves is neglected; see [Achenbach 1976; Ewing et al. 1957] for more detail. The ranges of validity of such assumptions are evaluated in what follows.

3. Point contact

Consider first a plane time-harmonic problem in cartesian coordinates (x_1, x_3). For a point contact, we get from (2-1) at $P = -P_0\delta(x_1)e^{-i\omega t}$ in its right-hand side

$$\frac{\partial^2 \varphi}{\partial x_1^2} - \frac{1}{c_R^2}\frac{\partial^2 \varphi}{\partial t^2} = -\frac{1 + k_2^2}{2\mu B}P_0\delta(x_1)e^{-i\omega t}, \tag{3-1}$$

where ω is angular frequency, P_0 is constant amplitude of normal stress, and $\delta(x_1)$ denotes the Dirac-delta function. The solution of this equation is

$$\varphi(x_1, 0, t) = i\frac{1 + k_2^2}{4\mu B}\frac{P_0 c_R}{\omega}e^{i\omega(|x_1|/c_R - t)}, \tag{3-2}$$

corresponding to propagating surface Rayleigh wave patterns.

Next, we apply a Fourier transform in x_1 to the 2D counterpart of the elliptic equation (2-2) over the interior, having

$$\frac{d^2\varphi^F}{dx_3^2} - k_1^2 k^2 \varphi^F = 0, \tag{3-3}$$

where φ^F denotes the transformed potential and k is Fourier transform parameter. Its solution can be written as

$$\varphi^F(k, x_3, t) = \frac{1 + k_2^2}{2\mu B}\frac{P_0}{k^2 - \omega^2/c_R^2}e^{-k_1|k|x_3 - i\omega t}. \tag{3-4}$$

As a result,

$$\varphi(x_1, x_3, t) = \frac{(1 + k_2^2)P_0 e^{-i\omega t}}{4\pi\mu B}\int_{-\infty}^{\infty}\frac{e^{-k_1|k|x_3}}{k^2 - \omega^2/c_R^2}e^{-ikx_1}\,dk. \tag{3-5}$$

Let us now split the integral in (3-5) into two parts as

$$\int_{-\infty}^{\infty}\frac{e^{-k_1|k|x_3}}{k^2 - \omega^2/c_R^2}e^{-ikx_1}\,dk = I_1 + I_2, \tag{3-6}$$

where

$$I_1 = \frac{c_R}{2\omega}\int_{-\infty}^{\infty}\left(\frac{e^{-k_1\omega x_3/c_R}}{k - \omega/c_R} - \frac{e^{-k_1\omega x_3/c_R}}{k + \omega/c_R}\right)e^{-ikx_1}\,dk \tag{3-7}$$

and

$$I_2 = \frac{c_R}{\omega}\int_0^{\infty}\left(\frac{e^{-k_1kx_3} - e^{-k_1\omega x_3/c_R}}{k - \omega/c_R} - \frac{e^{-k_1kx_3} - e^{-k_1\omega x_3/c_R}}{k + \omega/c_R}\right)\cos(kx_1)\,dk. \tag{3-8}$$

The integral I_2 has no poles and can be readily evaluated numerically. As for the integral I_1, it accounts for the contribution of the Rayleigh wave poles and takes the form

$$I_1(x_1, x_3) = \frac{i\pi c_R}{\omega}e^{(i|x_1| - k_1 x_3)\omega/c_R}. \tag{3-9}$$

It is worth noting that the last formula, due to the presence of $|x_1|$, demonstrates a discontinuity of the derivative with respect to x_1 at $x_1 = 0$ not only at the surface $x_3 = 0$ but also over the interior $x_3 > 0$. However, this is also a feature of the Rayleigh pole contribution to the exact solution of the
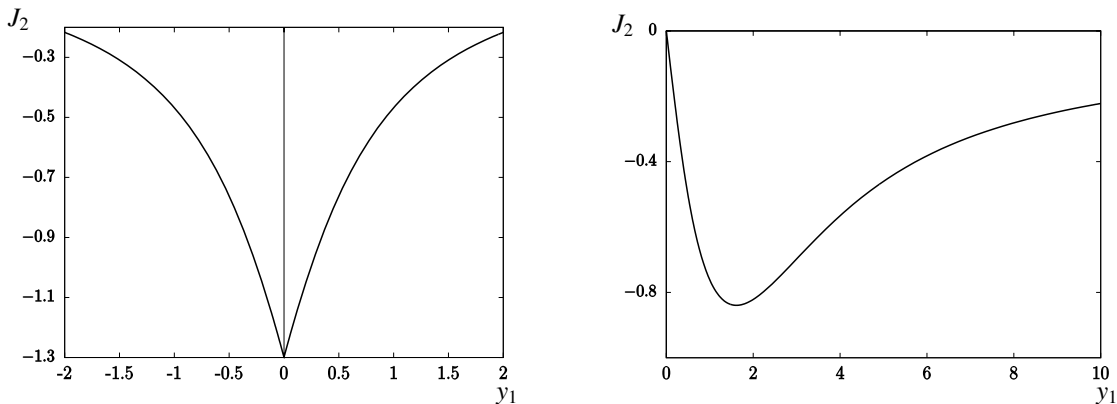
Figure 3. Variation of the integral J_2 along the horizontal and vertical axes for $\nu = 0.25$ and $c_R = 0.914 c_2$. Left: $y_3 = 1$. Right: $y_1 = 0$.

associated plane problem in elasticity presented in the Appendix. In fact, calculating the aforementioned contribution φ_1 to integral (A-5), we have

$$\varphi_1(x_1, x_3, t) = \frac{(1 + k_2^2) P_0}{\pi \mu R'(c_R/c_2)} \frac{c_2}{c_R} I_1(x_1, x_3) e^{-i\omega t}, \tag{3-10}$$

where the Rayleigh denominator is defined by (A-10). It can easily be verified that

$$R'(c_R/c_2) = 4B \, c_2/c_R, \tag{3-11}$$

with constant B from (2-1). Thus, the approximation of the surface wave field given by formulae (3-5) with (3-9) and (3-10) coincide.

At the same time, the integral I_2 is a spurious product of the utilized model for the surface Rayleigh wave, which does not appear in the exact solution of the problem. It corresponds to a pattern localized near a point contact and arises in the model due to neglecting the integrals over the branch cuts characteristic of the exact formulation, e.g., see [Achenbach 1976; Ewing et al. 1957]. This integral may be rewritten in the form

$$I_2 = \frac{\omega}{c_R} J_2 \tag{3-12}$$

with

$$J_2 = \int_0^\infty \left(\frac{e^{-k_1 \zeta y_3} - e^{-k_1 c_2/c_R y_3}}{\zeta - c_2/c_R} - \frac{e^{-k_1 \zeta y_3} - e^{-k_1 c_2/c_R y_3}}{\zeta + c_2/c_R} \right) \cos(\zeta y_1) \, d\zeta, \tag{3-13}$$

where $y_i = \omega/c_2 \, x_i$, $i = 1, 3$. It is plotted in Figure 3 for the Poisson ratio $\nu = 0.25$ and consequently with the Rayleigh wave speed $c_R = 0.914 c_2$ for $y_1 = 0$ (Figure 3, left) and $y_3 = 1$ (Figure 3, right).

The spurious component of the solution related to the integral J_2 makes more problematic the applicability of the promoted surface wave model for tackling a point contact. Moreover, the latter cannot also be treated in the general framework of linear elasticity. In the latter case, the vertical displacement u_3 does not take a finite value at the origin $x_1 = x_3 = 0$ because of the divergence of a Fourier integral following from (A-5), (A-6), and (2-5); see [Ewing et al. 1957] for more detail. In literature, the problem is usually overcome by distributing a point contact, e.g., see [Satto and Wada 1977].

4. Array of mass-spring oscillators

Consider now a plane strain problem for a regular array of mass-spring oscillators attached to the surface of the half-space $x_3 = 0$; see Figure 4. Let m represent mass, χ the spring stiffness, and a the distance between the oscillators. Then, we have from the general equation (2-1),

$$\frac{\partial^2 \varphi}{\partial x_1^2} - \frac{1}{c_R^2} \frac{\partial^2 \varphi}{\partial t^2} = -\frac{1 + k_2^2}{2\mu B} \sum_{n=-\infty}^{\infty} p(x_1, t)\delta(x_1 + na), \tag{4-1}$$

where p is a contact force. In this case, the original 3D elliptic equations for the interior in Section 2 become

$$\frac{\partial^2 \varphi}{\partial x_3^2} + k_1^2 \frac{\partial^2 \varphi}{\partial x_1^2} = 0, \tag{4-2}$$

$$\frac{\partial^2 \psi}{\partial x_3^2} + k_2^2 \frac{\partial^2 \psi}{\partial x_1^2} = 0, \tag{4-3}$$

where $\varphi = \varphi(x_1, x_3, t)$ and $\psi = \psi(x_1, x_3, t)$ with $\psi_i = \psi$, $i = 1, 2$. The relation between the potentials now takes the form

$$\frac{\partial \psi}{\partial x_3} = \frac{1 + k_2^2}{2} \frac{\partial \varphi}{\partial x_1}. \tag{4-4}$$

We also need the formula for the vertical displacement:

$$u_3 = \frac{\partial \varphi}{\partial x_3} + \frac{\partial \psi}{\partial x_1}. \tag{4-5}$$

Let the vibration of each of the oscillators be governed by

$$m v_{tt} + \chi v = p. \tag{4-6}$$

In addition, we impose the continuity of vertical displacements; see (2-7)$_2$.

First, we distribute the contact stress in the right-hand side of (4-1), setting

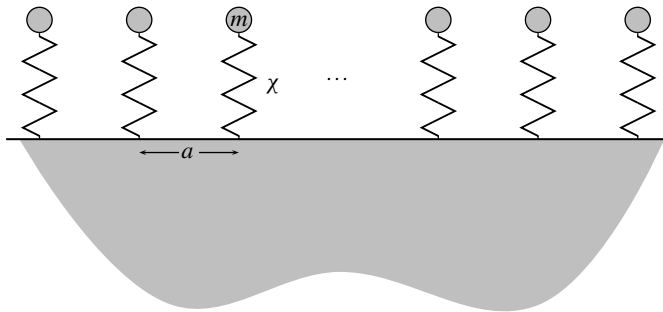$$\sum_{n=-\infty}^{\infty} p(x_1, t)\delta(x_1 + na) \approx \frac{1}{a} p(x_1, t). \tag{4-7}$$

Figure 4. Array of mass-spring oscillators.

Thus, a typical wavelength is assumed to be much greater than the distance between the oscillators. A more sophisticated homogenization technique for a regular array of oscillators is reported in [Boutin and Roussillon 2006].

For a time-harmonic wave in the form $p = p_0 \exp i(kx_1 - \omega t)$, where p_0 is a constant, k is the wavenumber, and ω is the frequency, we readily obtain from equations (4-2)–(4-5)

$$\varphi = -\frac{A}{kk_1} e^{i(kx_1 - \omega t) - kk_1 x_3} \tag{4-8}$$

and

$$\psi = \frac{2iA}{k(1+k_2^2)} e^{i(kx_1 - \omega t) - kk_2 x_3}, \tag{4-9}$$

where A is an unknown amplitude. As a result, (4-6) yields

$$v = \frac{p_0}{m(\omega_0^2 - \omega^2)} e^{i(kx_1 - \omega t)} \tag{4-10}$$

with

$$\omega_0 = \sqrt{\chi/m}. \tag{4-11}$$

We also have from (4-5)

$$u_3 = A\left(e^{-kk_1 x_3} - \frac{2e^{-kk_2 x_3}}{1+k_2^2} \right) e^{i(kx_1 - \omega t)}. \tag{4-12}$$

On substituting formulae (4-8), (4-10), and (4-12) into the wave equation (4-1) and the continuity condition (2-7)$_2$, we arrive at linear algebraic equations with unknowns A and p_0. They are

$$(k^2 - \omega^2/c_R^2)A = \frac{(1+k_2^2)kk_1}{2\mu aB} p_0, \tag{4-13}$$

$$\frac{1-k_2^2}{1+k_2^2} A = \frac{1}{m(\omega^2 - \omega_0^2)} p_0. \tag{4-14}$$

The associated dispersion relation can be presented as

$$K^2 - \Omega^2 = r(s^2\Omega^2 - 1)K, \tag{4-15}$$

where the dimensionless wave number and frequency are given by

$$K = ka, \quad \Omega = \frac{\omega a}{c_R} \tag{4-16}$$

and

$$s = \frac{c_R}{\omega_0 a}, \quad r = \frac{(1-k_2^2)k_1 \chi}{2\mu B}. \tag{4-17}$$

The zero of the left-hand side in (4-15), $K = \Omega$, corresponds to the Rayleigh surface wave, whereas its right-hand side zero, $\Omega_0 = s^{-1}$, coincides with the eigenfrequency of the considered oscillator. The exploited surface wave model is formally valid near the left-hand side zero, e.g., see [Kaplunov and Prikazchikov 2017], and it becomes exact at $K_0 = s^{-1}$.
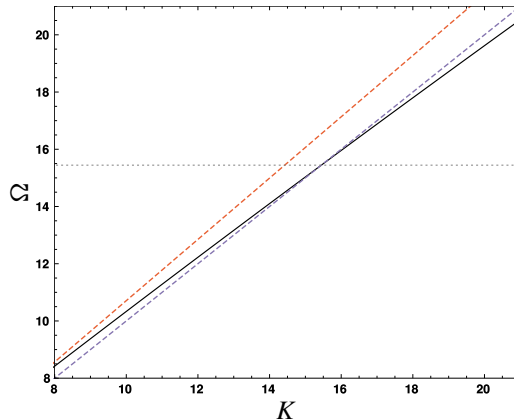
Figure 5. Dispersion curve for an array of mass-spring oscillators. The dispersion equation (4-18) is plotted by a black line, the shear wave ($K = \Omega$) is plotted by the red dotted line, and the Rayleigh wave ($K = c_2/c_R \, \Omega$) is plotted by the blue dotted line.

Numerical results are presented in Figure 5, where the dispersion curve calculated by the formula

$$K = \frac{r(s^2\Omega^2 - 1) + \sqrt{r^2(s^2\Omega^2 - 1)^2 + 4\Omega^2}}{2} \tag{4-18}$$

is plotted by solid line. In this figure, $m = 1000 \, \text{kg/m}$, $a = 2 \, \text{m}$, $\mu = 325 \, \text{MPa}$, $\chi = 4 \, \mu$, $c_1 = 232.379 \, \text{m/s}$, $c_2 = 158.114 \, \text{m/s}$, and $c_R = 140.109 \, \text{m/s}$. The Rayleigh wave $K = c_2/c_R \, \Omega$ (blue dotted line) and shear wave $K = \Omega$ (red dotted line) are also shown along with the eigenfrequency Ω_0 (horizontal line). The figure demonstrates that the validity range of the model is located near the point with coordinates (K_0, Ω_0).

5. Array of elastic rods

In this section, we study a more elaborate plane time-harmonic problem for an array of elastic rods of height H and width h; see Figure 6. We start from the relations in the previous sections using, instead of (4-6), the boundary value problem for longitudinal vibration of a rod over the interval $-H \leq x_3 \leq 0$. This is given by the equation

$$E \frac{\partial^2 v}{\partial x_3^2} - m \frac{\partial^2 v}{\partial t^2} = 0, \tag{5-1}$$

subject to the boundary conditions

$$\frac{\partial v}{\partial x_3} = \frac{p}{Eh}, \quad x_3 = 0, \tag{5-2}$$

$$\frac{\partial v}{\partial x_3} = 0, \qquad x_3 = -H, \tag{5-3}$$

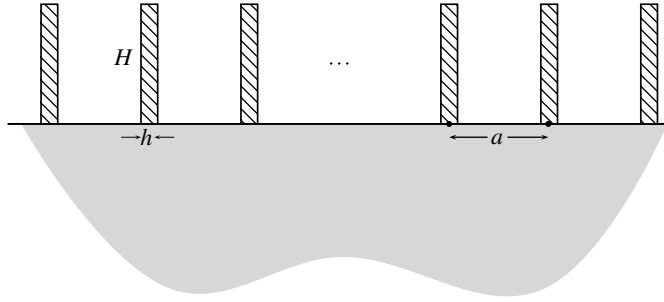where m and E are the mass density and Young's modulus, respectively.

Figure 6. Array of elastic rods.

The solution of the problem (5-1)–(5-3) is

$$v = -\frac{c_0 p}{E h \omega} \frac{\cos(\omega(x_3 + H)/c_0)}{\sin(\omega H / c_0)}, \tag{5-4}$$

with

$$c_0 = \sqrt{E/m}. \tag{5-5}$$

The continuity of the displacements at $x_3 = 0$, see (2-7), taking into account (4-12), results in

$$\frac{c_0}{\omega} \cot \frac{\omega H}{c_0} p_0 = \frac{1 - k_2^2}{1 + k_2^2} A. \tag{5-6}$$

The compatibility of the linear homogeneous equations (5-6) and (4-13) leads to the dispersion relation

$$K^2 - \Omega^2 = q \theta_h K \Omega \tan(\theta_H \Omega), \tag{5-7}$$

where K and Ω are given by (4-16) as above and

$$\theta_h = \frac{c_R h}{c_0 a}, \quad \theta_H = \frac{c_R H}{c_0 a}, \quad q = \frac{E k_1 (1 - k_2^2)}{2 \mu B}. \tag{5-8}$$

The zeros of the right-hand side in (5-7),

$$\Omega_m = \frac{\pi m}{\theta_H}, \quad m = 1, 2, 3, \ldots, \tag{5-9}$$

correspond to the eigenfrequencies of a rod with free ends, for which $p = 0$ in (5-2). At the same time, its poles,

$$\Omega_m = \frac{\pi}{2 \theta_H} (2m - 1), \quad m = 1, 2, 3, \ldots, \tag{5-10}$$

are related to a rod with a clamped end at $x_3 = 0$. In this case we have to impose the boundary condition $v = 0$ instead of (5-2).

The exact solution of the studied problem in [Colquitt et al. 2017] rewritten in the notation of the present paper becomes

$$R\left(\frac{c_R}{c_2} \frac{\Omega}{K}\right) = -\frac{2Bq\theta_h}{k_1} \left(\frac{\Omega}{K}\right)^3 \sqrt{1 - \frac{c_R^2}{c_1^2} \frac{\Omega^2}{K^2}} \tan(\theta_H \Omega), \tag{5-11}$$
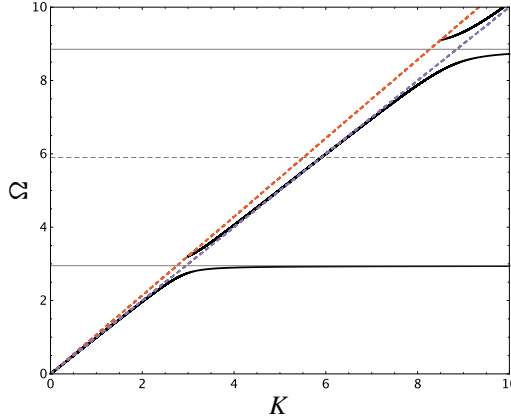
Figure 7. Dispersion curves for the array of rods. Black solid lines correspond to the approximate dispersion equation (5-14) with eigenfrequencies (5-9) and (5-10) indicated by the horizontal dashed and solid lines respectively.

where the Rayleigh denominator R is defined in the Appendix; see (A-10). Its one-term Taylor expansion around $\Omega = K$ is given by

$$R\left(\frac{c_R}{c_2}\frac{\Omega}{K}\right) \approx \frac{c_R}{c_2}\frac{R'(c_R/c_2)}{2K^2}(\Omega^2 - K^2). \tag{5-12}$$

Then, on substituting the latter into the exact dispersion relation (5-11) and taking into consideration identity (3-11), we arrive at

$$K^2 - \Omega^2 = \frac{q\theta_h}{k_1}\frac{\Omega^3}{K}\sqrt{1 - \frac{c_R^2}{c_1^2}\frac{\Omega^2}{K^2}}\ \tan(\theta_H\Omega). \tag{5-13}$$

As might be expected, the right-hand sides of dispersion relations (5-7) and (5-13) are identical at $\Omega = K$, i.e., for the Rayleigh wave.

Numerical data are given in Figures 7 and 8 for the parameters of rods $E = 1.7\,\text{GPa}$, $m = 450\,\text{kg}\cdot\text{m}^{-3}$, $H = 14\,\text{m}$, and $h = 0.3\,\text{m}$ with the same distance between the oscillators and the same parameters of the half-space as in the previous section. For the surface wave model, the dispersion curves are calculated starting from the explicit formula

$$K = \frac{q\theta_h\Omega\tan(\theta_H\Omega) + \sqrt{q^2\theta_h^2\Omega^2\tan^2(\theta_H\Omega) + 4\Omega^2}}{2}, \tag{5-14}$$

while the curves originating from the exact solution are plotted from the transcendental equation (5-11). Since the curves corresponding to (5-11) and (5-14) are virtually identical, in Figure 7, only the approximate dispersion equation is plotted by solid black lines. Eigenfrequency (5-9) and (5-10) are shown in this figure by dashed and solid horizontal lines, respectively. As before, the Rayleigh and shear waves are also displayed. In Figure 8, the curves by (5-11) and (5-14) are depicted by blue and black lines, respectively. It is worth noting that the adapted approximate model also demonstrates a reasonable accuracy near the
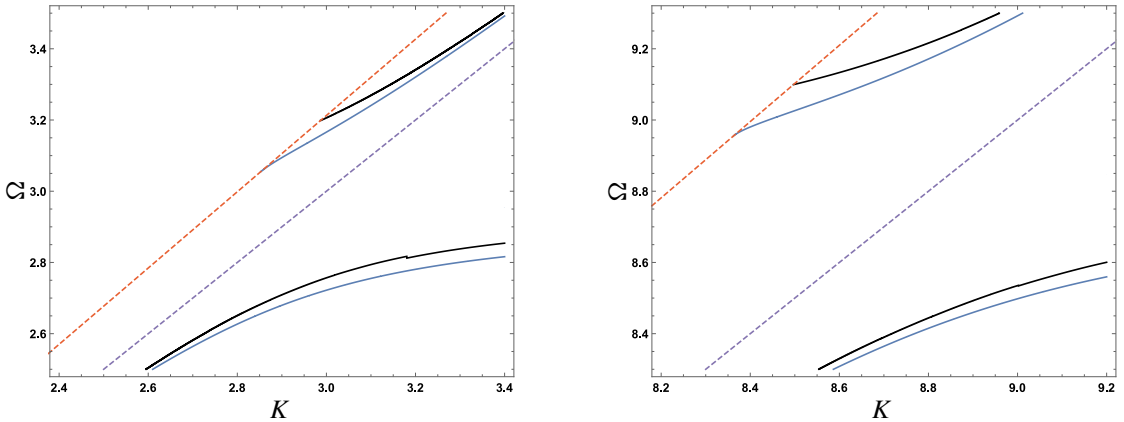
Figure 8. Comparison of the formula (5-14) and the dispersion relation (5-11), corresponding to black and blue solid lines respectively, near the first (left) and second (right) band-gaps.

band-gaps centred around frequencies (5-10) related to a clamped surface of the half-space, which does not support Rayleigh wave propagation.

6. Concluding remarks

An approximate scheme starting from the explicit model for the Rayleigh wave, e.g., see [Kaplunov and Prikazchikov 2017], has been developed for surface wave-structure interaction problems. This scheme is proven not valid for analysing a point harmonic contact. As a result, its various extensions aimed at taking into consideration contact stresses distributed over small surface regions, for example using the methodology in [Muravskii 2008], seem to be of obvious interest.

Comparison with the exact solution of the plane time-harmonic problem for an array of elastic rods attached to the surface demonstrates an acceptable accuracy of the scheme, see Figures 7 and 8, which gives a notable prediction even near band-gaps. In this case, there is also a potential for applying advanced homogenization techniques, as has been done in [Boutin and Roussillon 2006]. Overall, a very promising outcome of the presented comparison indicates clear prospects for implementing the scheme in more elaborated problems of surface wave-structure interaction inspired by the modelling of seismic metasurfaces [Colombi et al. 2016; Colquitt et al. 2017] and also calculating the seismic response of wind turbines and farms, e.g., see [Saccorotti et al. 2011; Westwood et al. 2015].

Appendix

A.1. *Plane problem in elasticity for a half-space.* Consider the plane time-harmonic problem in elasticity for a half-space $-\infty < x_1, x_2 < \infty, 0 < x_3 < \infty$ subject to the following boundary conditions at $x_3 = 0$:

$$\sigma_{13} = \mu \left(2 \frac{\partial^2 \varphi}{\partial x_1 \partial x_3} + \frac{\partial^2 \psi_1}{\partial x_1^2} - \frac{\partial^2 \psi_2}{\partial x_3^2} \right) = 0, \tag{A-1}$$

$$\sigma_{33} = \lambda\left(\frac{\partial^2\varphi}{\partial x_1^2} + \frac{\partial^2\varphi}{\partial x_3^2}\right) + 2\mu\left(\frac{\partial^2\varphi}{\partial x_3^2} + \frac{\partial^2\psi}{\partial x_1 x_3}\right) = -P_0\delta(x_1)e^{-i\omega t}, \tag{A-2}$$

where λ and μ are Lamé parameters, and the wave potentials φ and ψ satisfy the equations

$$\frac{\partial^2\varphi}{\partial x_1^2} + \frac{\partial^2\varphi}{\partial x_3^2} - \frac{1}{c_1^2}\frac{\partial^2\varphi}{\partial t^2} = 0, \tag{A-3}$$

$$\frac{\partial^2\psi}{\partial x_1^2} + \frac{\partial^2\psi}{\partial x_3^2} - \frac{1}{c_2^2}\frac{\partial^2\psi}{\partial t^2} = 0. \tag{A-4}$$

The solution of the formulated problem expressed through Fourier integrals takes the form, e.g., see [Achenbach 1976],

$$\varphi(x_1, x_3, t) = -\frac{P_0 e^{-i\omega t}}{2\pi\mu}\int_{-\infty}^{\infty}\frac{2k^2 - \omega^2/c_2^2}{F}e^{-ikx_1 - \alpha_1 x_3}\,dk, \tag{A-5}$$

and

$$\psi(x_1, x_3, t) = -\frac{P_0 e^{-i\omega t}}{2\pi\mu}\int_{-\infty}^{\infty}\frac{2ik\alpha_1}{F}e^{-ikx_1 - \alpha_2 x_3}\,dk, \tag{A-6}$$

where

$$F = (2k^2 - \omega^2/c_2^2)^2 - 4k^2\alpha_1\alpha_2 \tag{A-7}$$

and

$$\alpha_i = \sqrt{k^2 - \omega^2/c_i^2}, \quad i = 1, 2. \tag{A-8}$$

The function F can be written as

$$F(k, \omega) = k^4 R(c), \tag{A-9}$$

where R is the well-known Rayleigh denominator given by

$$R(c) = (2 - c^2)^2 - 4\sqrt{1 - c^2}\sqrt{1 - \gamma^2 c^2}, \tag{A-10}$$

where $c = \omega/(kc_2)$ and

$$\gamma = \sqrt{\frac{c_2}{c_1}} = \sqrt{\frac{1 - 2\nu}{2 - 2\nu}}, \tag{A-11}$$

with ν denoting the Poisson's ratio.

References

[Achenbach 1976] J. D. Achenbach, *Wave propagation in elastic solids*, 1st ed., North-Holland Series in Applied Mathematics and Mechanics **16**, North-Holland Publishing Co., Amsterdam, 1976.

[Boutin and Roussillon 2004] C. Boutin and P. Roussillon, "Assessment of the urbanization effect on seismic response", *Bull. Seismol. Soc. Am.* **94**:1 (2004), 251–268.

[Boutin and Roussillon 2006] C. Boutin and P. Roussillon, "Wave propagation in presence of oscillators on the free surface", *Int. J. Eng. Sci.* **44**:3-4 (2006), 180–204.

[Colombi et al. 2016] A. Colombi, P. Roux, S. Guenneau, P. Gueguen, and R. V. Craster, "Forests as a natural seismic metamaterial: Rayleigh wave bandgaps induced by local resonances", *Scientific Reports* **6** (2016), art. id. 19238.

[Colquitt et al. 2017] D. J. Colquitt, A. Colombi, R. V. Craster, P. Roux, and S. R. L. Guenneau, "Seismic metasurfaces: sub-wavelength resonators and Rayleigh wave interaction", *J. Mech. Phys. Solids* **99** (2017), 379–393.

[Erbaş et al. 2017] B. Erbaş, J. Kaplunov, D. A. Prikazchikov, and O. Şahin, "The near-resonant regimes of a moving load in a three-dimensional problem for a coated elastic half-space", *Math. Mech. Solids* **22**:1 (2017), 89–100.

[Ewing et al. 1957] W. M. Ewing, W. S. Jardetzky, and F. Press, *Elastic waves in layered media*, McGraw-Hill, 1957.

[Kaplunov and Prikazchikov 2013] J. Kaplunov and D. A. Prikazchikov, "Explicit models for surface, interfacial and edge waves", pp. 73–114 in *Dynamic Localization Phenomena in Elasticity, Acoustics and Electromagnetism*, edited by R. V. Craster and J. Kaplunov, Springer, 2013.

[Kaplunov and Prikazchikov 2017] J. Kaplunov and D. A. Prikazchikov, "Asymptotic theory for Rayleigh and Rayleigh-type waves", pp. 1–106 Advances in Applied Mechanics **50**, Elsevier, 2017.

[Kaplunov et al. 2013] J. Kaplunov, D. A. Prikazchikov, B. Erbaş, and O. Şahin, "On a 3D moving load problem for an elastic half space", *Wave Motion* **50**:8 (2013), 1229–1238.

[Luco 1982] J. E. Luco, "Linear soil-structure interaction: a review", pp. 41–57 in *Earthquake ground motion and its effects on structures: Proc. of the Winter Annu. Meet. of the ASME* (Phoenix, AZ, 1982), edited by S. K. Datta, Applied Mechanics Division **53**, ASME, 1982.

[Muravskii 2008] G. B. Muravskii, "On simplified solutions of contact problems for elastic foundations", *Arch. Appl. Mech.* **78**:2 (2008), 149–162.

[Saccorotti et al. 2011] G. Saccorotti, D. Piccinini, L. Cauchie, and I. Fiori, "Seismic noise by wind farms: a case study from the Virgo gravitational wave observatory, Italy", *Bull. Seismol. Soc. Am.* **101**:2 (2011), 568–578.

[Satto and Wada 1977] H. Satto and H. Wada, "Forced vibrations of a mass connected to an elastic half-space by an elastic rod or a spring", *J. Sound Vib.* **50**:4 (1977), 519–532.

[Westwood et al. 2015] R. F. Westwood, P. Styles, and S. M. Toon, "Seismic monitoring and vibrational characterization of small wind turbines: a case study of the potential effects on the Eskdalemuir International Monitoring System Station in Scotland", *Near Surface Geophysics* **13**:2 (2015), 115–126.

[Wolf 1985] J. Wolf, *Dynamic soil-structure interaction*, Prentice-Hall, Englewood Cliffs, NJ, 1985.

NIHAL EGE: nsahin@anadolu.edu.tr
Department of Mathematics, Anadolu University, Eskisehir, Turkey

BARIŞ ERBAŞ: erbas.baris@gmail.com
Department of Mathematics, Anadolu University, Yunusemre Campus, Eskisehir, Turkey

JULIUS KAPLUNOV: j.kaplunov@keele.ac.uk
School of Computing and Mathematics, Keele University, Keele, United Kingdom

PETER WOOTTON: p.t.wootton@keele.ac.uk
School of Computing and Mathematics, Keele University, Keele, United Kingdom

JOURNAL OF MECHANICS OF MATERIALS AND STRUCTURES

msp.org/jomms

Founded by Charles R. Steele and Marie-Louise Steele